Water Clusters Induced Assembly of Chiral Organic Microstructures Showing Reversible Phase Transformations and Luminescence Switching

Guozan Yuan, Chengfeng Zhu, Yan Liu, Yu Fang and Yong Cui*

School of Chemistry and Chemical Technology, Shanghai Jiao Tong University, State Key Laboratory of Metal Matrix Composites, Shanghai 200240, China;

Email: yongcui@sjtu.edu.cn

Table of Content

1. Experimental Section

The synthesis and characterization of *R*-**1** can be found in our recent paper (Yuan et al. *J. Am. Chem. Soc.* **2009**, 131, 10452-10460). Tetrahydrofuran (THF)，MeOH，N, N-dimethylformide(DMF) , acetone and EtOH were obtained from Sinopharm Chemical Reagent Co., LtdS. Powder X-ray diffraction (PXRD) data were collected on a DMAX2500 diffractometer using Cu Kα radiation. The calculated PXRD patterns were produced using Mercury program. All UV/Vis absorption spectrum were recorded on a shimadzu UV-2450 Spectrometer. All fluorescence measurements were carried out on a Hitachi F-4500 Luminescence Spectrometer [We reported the PL of **1** in our recent paper (*J. Am. Chem. Soc.*, **2009**, 131, 10452-10460), but the data was later found to be due to the hydrated sample of **1** for a long exposure to air). The morphologies of the samples were characterized by field-emission scanning electron microscopy (FE-SEM; JEOL, JSM-6700F with an accelerating voltage of 1 kV). ^{1}H NMR experiments were carried out on a MERCURYplus 400 spectrometer operating at resonance frequencies of 100.63 MHz.

X-ray Crystallography. Single-crystal XRD data for the compounds was collected on a Bruker APEX II diffractometer with Mo-Kα radiation (λ = 0.71073 Å) at 123 K. The empirical absorption correction was applied by using the SADABS program (G. M. Sheldrick, SADABS, program for empirical absorption correction of area detector data; University of Göttingen, Göttingen, Germany, 1996). The structure was solved using direct method, and refined by full-matrix least-squares on *F*2 (G. M. Sheldrick, SHELXTL97, program for crystal structure refinement, University of Göttingen, Germany, 1997). All non-H atoms were refined anisotropically. Crystal data and details of the data collection are given in Table S1. The selected bond distances and angles are presented in Tables S2. CCDC-747373 contains the supplementary crystallographic data for this paper. These data can be obtained free of charge from the Cambridge Crystallographic Data Centre via www.ccdc.cam.ac.uk/data request/cif.

Preparation of the microstructures

(a) Preparation of microtubules

R-**1** was dissolved in MeOH to a concentration of 1×10^{-2} M, 8×10^{-3} M, 4×10^{-3} M, and 1×10^{-3} M respectively. 0.5 ml of each solution was injected into high-purity water (2 mL) with vigorous stirring. After stirring 3 min, the sample was left undisturbed for about 8 h to stabilize the microstructures. The sizes and shapes of the microtubules were observed with a field-emission scanning electron microscope (FESEM, JSM-7401F) operated at an accelerating voltage of 5 kV. For SEM studies, a few

drops of the sample were placed on a aluminum foil substrate and the solvent was left to evaporate. To minimize sample charging, the dried samples were coated with an ultra-thin layer of Au right before SEM examination.

(b) Preparation of microspheres

A solution of *R*-**1** in methanol (8×10^{-3} M, 0.5 mL) was injected into high-purity water (2 mL) with vigorous stirring. Instantly, the solution was evaporated on the aluminum foil in a short period of time. The shapes of the microspheres were observed with a field-emission scanning electron microscope (FESEM, JSM-7401F) operated at an accelerating voltage of 5 kV. For SEM studies, a few drops of the sample were placed on a aluminum foil substrate and the solvent was left to evaporate. To minimize sample charging, the dried samples were coated with an ultra-thin layer of Au right before SEM examination.

(c) Preparation of microleaves

R-**1** was dissolved in MeOH to a concentration of 4×10^{-3} M . 0.5 ml of these solution was injected into high-purity water (2 mL) with vigorous stirring. After stirring 3 min, the sample was left undisturbed for about 8 h to stabilize the microstructures. The shapes of the microleaves were observed with a field-emission scanning electron microscope (FESEM, FEI SIRION 200) operated at an accelerating voltage of 5 kV. For SEM studies, a few drops of the sample were placed on a aluminum foil substrate and the solvent was left to evaporate. To minimize sample charging, the dried samples were coated with an ultra-thin layer of Au right before SEM examination.

2. Table S1. Crystal data and structure refinement for *R*-**1**·2H_2O and Racemic-**1**

Identification code	*R*-**1**·2H_2O	Racemic-**1**
Empirical formula	$C_{28}H_{32}N_2O_4$	$C_{28}H_{28}N_2O_2$
Formula weight	460.56	424.52
Temperature (K)	123(2) K	296(2) K
Wavelength (Å)	0.71073	0.71073
Crystal system	orthorhombic	monoclinic
Space group	P2(1)2(1)2	C2/c
Unit cell dimensions	a = 12.366(5) Å b = 27.132(10) Å c = 7.849(3) Å α = 90° β = 90° γ = 90°	a = 18.2891(18) Å b = 6.7249(7) Å c = 19.162(2) Å α = 90° β = 98.169(2)° γ = 90°
Volume ($Å^3$), Z	2633.2(17), 4	2332.8(4), 4
Density (calculated) (mg/m^3)	1.162	1.209
Absorption coefficient (mm^{-1})	0.078	0.076
F(000)	984	904
θ range for data collection (º)	1.50 to 25.00	2.15 to 27.55
Limiting indices	$-13 \le h \le 14$ $-32 \le k \le 29$ $-9 \le l \le 9$	$-23 \le h \le 23$ $-8 \le k \le 5$ $-24 \le l \le 24$
Reflections collected	10876	9831
Independent reflections	4625 [R(int) = 0.0462]	2664 [R(int) = 0.0546]
Completeness to theta	25.00/99.1 %	27.55/98.6%
Refinement method	Full-matrix least-squares on F^2	Full-matrix least-squares on F^2
Data / restraints / parameters	4625 / 10/ 271	2664 / 0 / 146
Goodness-of-fit on F^2	0.924	1.035
Final R indices [I>2sigma(I)]	R1 = 0.0674, wR2 = 0.1739	R1 = 0.0610, wR2 = 0.1767
R indices (all data)	R1 = 0.1088, wR2 = 0.1927	R1 = 0.1129, wR2 = 0.2204
Largest diff. peak and hole ($e.Å^{-3}$)	0.311 and -0.282	0.332 and -0.305

3.1 **Tables S2.** Selected bond lengths (Å) and angles (º) for *R*-**1**·2H_2O

N(1)-C(1)	1.3900
N(1)-C(5)	1.3900
C(1)-C(2)	1.3900
C(2)-C(3)	1.3900
C(3)-C(4)	1.3900
C(3)-C(6)	1.538(5)
C(4)-C(5)	1.3900
C(12)-C(10)	1.510(10)
C(6)-C(7)	1.3900
C(6)-C(11)	1.3900
C(7)-C(8)	1.3900
C(7)-O(1)	1.407(6)
C(8)-C(9)	1.3900
C(8)-C(15)	1.496(4)
C(9)-C(10)	1.3900
C(9)-C(13)	1.491(10)
C(10)-C(11)	1.3900
C(14)-O(1)	1.421(9)
C(15)-C(16)	1.3900
C(15)-C(20)	1.3900
C(16)-C(17)	1.3900
C(16)-O(2)	1.407(6)
C(17)-C(18)	1.3900
C(17)-C(24)	1.529(6)
C(18)-C(19)	1.3900
C(19)-C(20)	1.3900
C(19)-C(22)	1.507(9)
C(20)-C(21)	1.5045
C(23)-O(2)	1.413(9)
C(24)-C(25)	1.3900
C(24)-C(28)	1.3900
C(25)-C(26)	1.3900
C(26)-N(2)	1.3900
N(2)-C(27)	1.3900
C(27)-C(28)	1.3900

C(1)-N(1)-C(5)	120.0
N(1)-C(1)-C(2)	120.0
C(3)-C(2)-C(1)	120.0
C(2)-C(3)-C(4)	120.0
C(2)-C(3)-C(6)	122.2(4)

C(4)-C(3)-C(6)	117.6(4)
C(5)-C(4)-C(3)	120.0
C(4)-C(5)-N(1)	120.0
C(10)-C(12)-H(12C)	109.5
C(7)-C(6)-C(11)	120.0
C(7)-C(6)-C(3)	122.7(4)
C(11)-C(6)-C(3)	116.9(4)
C(8)-C(7)-C(6)	120.0
C(8)-C(7)-O(1)	118.4(4)
C(6)-C(7)-O(1)	121.5(4)
C(7)-C(8)-C(9)	120.0
C(7)-C(8)-C(15)	119.1(4)
C(9)-C(8)-C(15)	120.9(4)
C(8)-C(9)-C(10)	120.0
C(8)-C(9)-C(13)	120.4(5)
C(10)-C(9)-C(13)	119.5(5)
C(11)-C(10)-C(9)	120.0
C(11)-C(10)-C(12)	117.5(5)
C(9)-C(10)-C(12)	122.5(5)
C(10)-C(11)-C(6)	120.0
C(16)-C(15)-C(20)	120.0
C(16)-C(15)-C(8)	118.5(3)
C(20)-C(15)-C(8)	121.5(3)
C(15)-C(16)-C(17)	120.0
C(15)-C(16)-O(2)	118.9(3)
C(17)-C(16)-O(2)	121.0(3)
C(16)-C(17)-C(18)	120.0
C(16)-C(17)-C(24)	120.9(3)
C(18)-C(17)-C(24)	119.0(3)
C(19)-C(18)-C(17)	120.0
C(20)-C(19)-C(18)	120.0
C(20)-C(19)-C(22)	121.8(5)
C(18)-C(19)-C(22)	118.2(5)
C(19)-C(20)-C(15)	120.0
C(19)-C(20)-C(21)	121.0
C(15)-C(20)-C(21)	118.9
C(25)-C(24)-C(28)	120.0
C(25)-C(24)-C(17)	121.0(4)
C(28)-C(24)-C(17)	118.9(4)
C(24)-C(25)-C(26)	120.0
N(2)-C(26)-C(25)	120.0
C(27)-N(2)-C(26)	120.0
N(2)-C(27)-C(28)	120.0
C(27)-C(28)-C(24)	120.0

C(7)-O(1)-C(14)	114.5(6)
C(16)-O(2)-C(23)	114.4(6)
H(31W)-O(3)-H(32W)	106(6)
H(41W)-O(4)-H(42W)	109(6)

4. Table S3. Hydrogen bonds for (Å) and angles (º) for *R*-**1**·2H_2O

D-H...A	d(D-H)	d(H...A)	d(D...A)	<(DHA)
O(4)-H(41W)...N(2)#2	0.95(4)	1.95(5)	2.90(3)	175(11)
O(3)-H(31W)...N(1)#3	0.96(4)	1.99(6)	2.851(8)	149(9)
O(4)-H(42W)...O(3)#4	0.96(4)	2.01(7)	2.840(12)	144(10)
O(3)-H(32W)...O(4)#1	0.96(4)	1.88(4)	2.842(12)	174(17)

Symmetry transformations used to generate equivalent atoms:
#1 x,y,z #2 x-1,y,z-1 #3 x,y,z+1 #4 -x+1,-y+1,z

5. Tables S4. Selected bond lengths (Å) and angles (º) for Racemic-**1**

O(1)-C(5)	1.388(3)
O(1)-C(15)	1.424(4)
C(2)-C(5)	1.394(3)
C(2)-C(6)	1.399(3)
C(2)-C(2)#1	1.507(4)
C(3)-C(4)	1.382(4)
C(3)-C(8)	1.390(3)
C(3)-H(3A)	0.9300
C(4)-C(5)	1.397(3)
C(4)-C(7)	1.496(3)
C(6)-C(8)	1.399(3)
C(6)-C(12)	1.505(3)
C(7)-C(14)	1.377(4)
C(7)-C(9)	1.390(3)
C(8)-C(10)	1.505(4)
C(9)-C(13)	1.375(4)
C(9)-H(9A)	0.9300
C(10)-H(10A)	0.9600
C(10)-H(10B)	0.9600
C(10)-H(10C)	0.9600
N(11)-C(13)	1.331(4)
N(11)-C(16)	1.331(4)

C(12)-H(12A)	0.9600
C(12)-H(12B)	0.9600
C(12)-H(12C)	0.9600
C(13)-H(13A)	0.9300
C(14)-C(16)	1.382(4)
C(14)-H(14A)	0.9300
C(15)-H(15A)	0.9600
C(15)-H(15B)	0.9600
C(15)-H(15C)	0.9600
C(16)-H(16A)	0.9300

C(5)-O(1)-C(15)	114.2(2)
C(5)-C(2)-C(6)	119.6(2)
C(5)-C(2)-C(2)#1	117.8(2)
C(6)-C(2)-C(2)#1	122.60(19)
C(4)-C(3)-C(8)	122.8(2)
C(4)-C(3)-H(3A)	118.6
C(8)-C(3)-H(3A)	118.6
C(3)-C(4)-C(5)	117.3(2)
C(3)-C(4)-C(7)	121.0(2)
C(5)-C(4)-C(7)	121.7(2)
O(1)-C(5)-C(2)	118.69(19)
O(1)-C(5)-C(4)	119.6(2)
C(2)-C(5)-C(4)	121.7(2)
C(8)-C(6)-C(2)	119.5(2)
C(8)-C(6)-C(12)	119.8(2)
C(2)-C(6)-C(12)	120.6(2)
C(14)-C(7)-C(9)	116.1(2)
C(14)-C(7)-C(4)	123.0(2)
C(9)-C(7)-C(4)	121.0(2)
C(3)-C(8)-C(6)	119.0(2)
C(3)-C(8)-C(10)	119.3(2)
C(6)-C(8)-C(10)	121.6(2)
C(13)-C(9)-C(7)	120.0(3)
C(13)-C(9)-H(9A)	120.0
C(7)-C(9)-H(9A)	120.0
C(8)-C(10)-H(10A)	109.5
C(8)-C(10)-H(10B)	109.5
H(10A)-C(10)-H(10B)	109.5
C(8)-C(10)-H(10C)	109.5
H(10A)-C(10)-H(10C)	109.5
H(10B)-C(10)-H(10C)	109.5
C(13)-N(11)-C(16)	115.2(3)
C(6)-C(12)-H(12A)	109.5

C(6)-C(12)-H(12B)	109.5
H(12A)-C(12)-H(12B)	109.5
C(6)-C(12)-H(12C)	109.5
H(12A)-C(12)-H(12C)	109.5
H(12B)-C(12)-H(12C)	109.5
N(11)-C(13)-C(9)	124.4(3)
N(11)-C(13)-H(13A)	117.8
C(9)-C(13)-H(13A)	117.8
C(7)-C(14)-C(16)	119.8(3)
C(7)-C(14)-H(14A)	120.1
C(16)-C(14)-H(14A)	120.1
O(1)-C(15)-H(15A)	109.5
O(1)-C(15)-H(15B)	109.5
H(15A)-C(15)-H(15B)	109.5
O(1)-C(15)-H(15C)	109.5
H(15A)-C(15)-H(15C)	109.5
H(15B)-C(15)-H(15C)	109.5
N(11)-C(16)-C(14)	124.6(3)
N(11)-C(16)-H(16A)	117.7
C(14)-C(16)-H(16A)	117.7

Symmetry transformations used to generate equivalent atoms:
#1 -x,y,-z+1/2

6.1 Figure S1. A view of the tetrameric water cluster in *R*-**1**·2H_2O showing hydrogen-bonding interactions, and (b) One of the twofold interpenetrated 2D supramolecular structure of *R*-**1**·2H_2O. (c) Twofold interpenetrated 2D supramolecular structure of *R*-**1**·2H_2O.

(a)

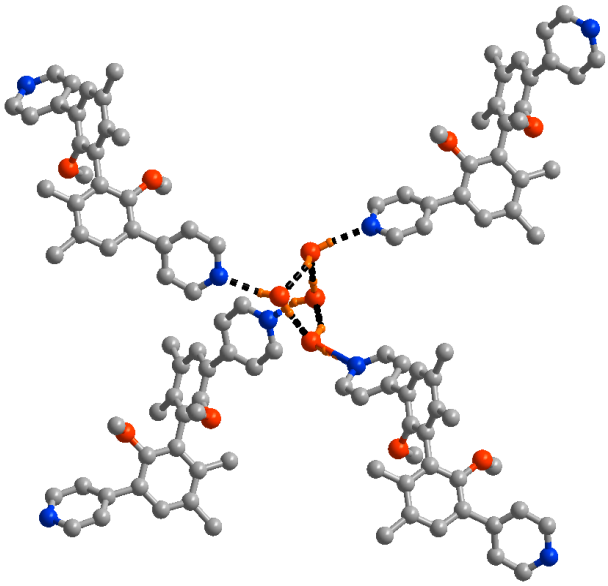

(b)

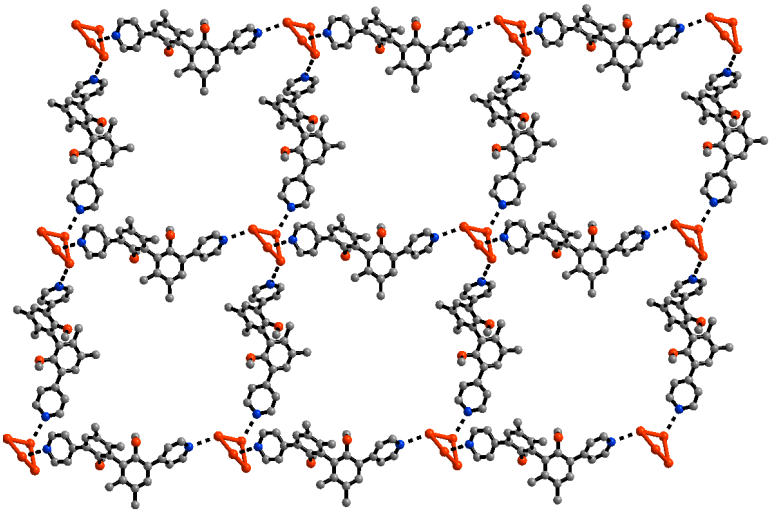

6.2 Figure S2. (a) This supramolecular structure of Racemic-**1** is stabilized by C-H…π interactions (C-H…π 3.33 and 3.37 Å) along the crystallographic *b*-axis; (b) View of Racemic-**1** structure along the crystallographic *b*-axis.

(a)

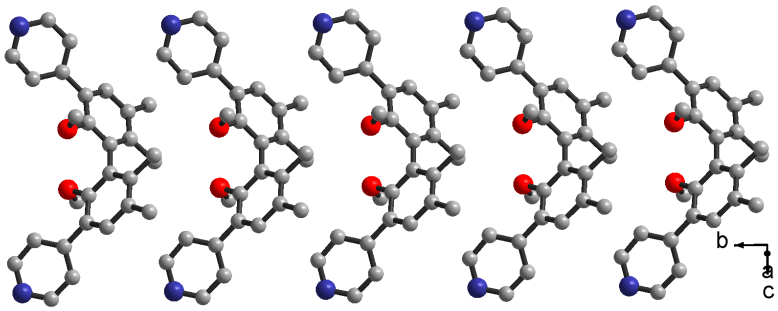

(b)

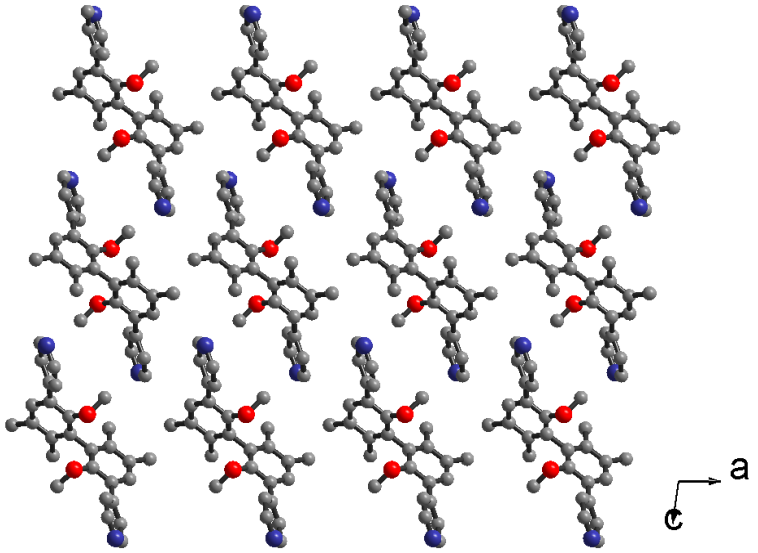

7.1 Figure S3. SEM images of *R*-**1**·2H_2O microtubules. The initial concentration of *R*-**1** is 4×10^{-3} M in MeOH.

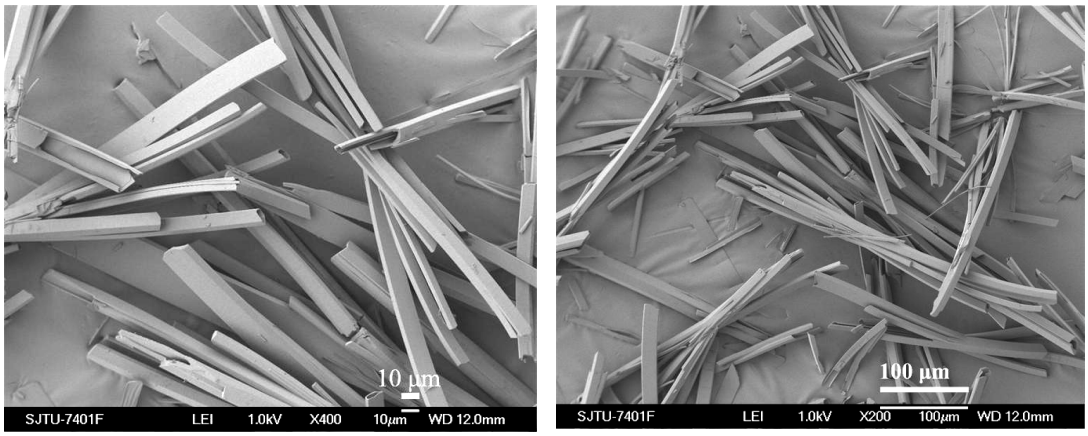

7.2. **Figure S4**. SEM image of *R*-**1**·2H_2O microtubules. The initial concentration of *R*-**1** is 1 ×10^{-2} M **i**n MeOH.

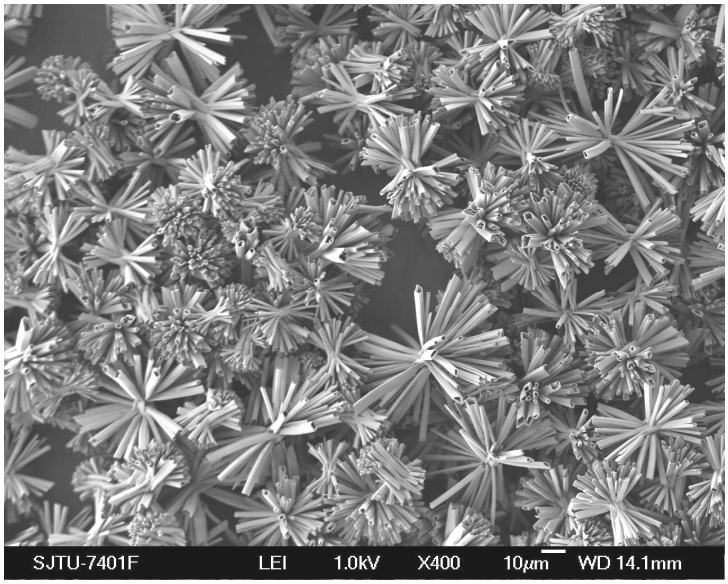

7.3 Figure S5. SEM image of *R*-**1**·2H_2O microspheres. The initial concentration of *R*-**1** is 8 ×10^{-3} M in MeOH.

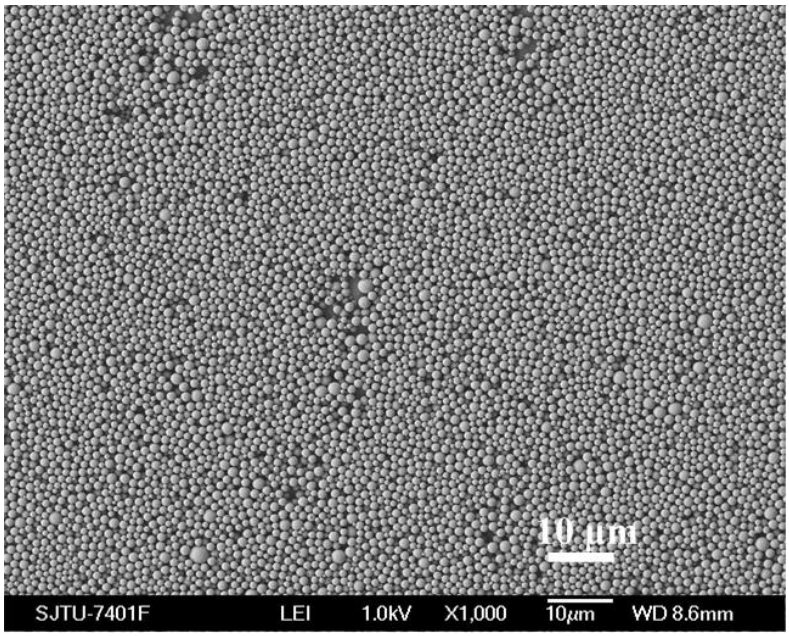

7.4 Figure S6. SEM image of *R*-**1**·$2H_2O$ microleaves. The initial concentration of *R*-**1** is 8×10^{-3} M in THF.

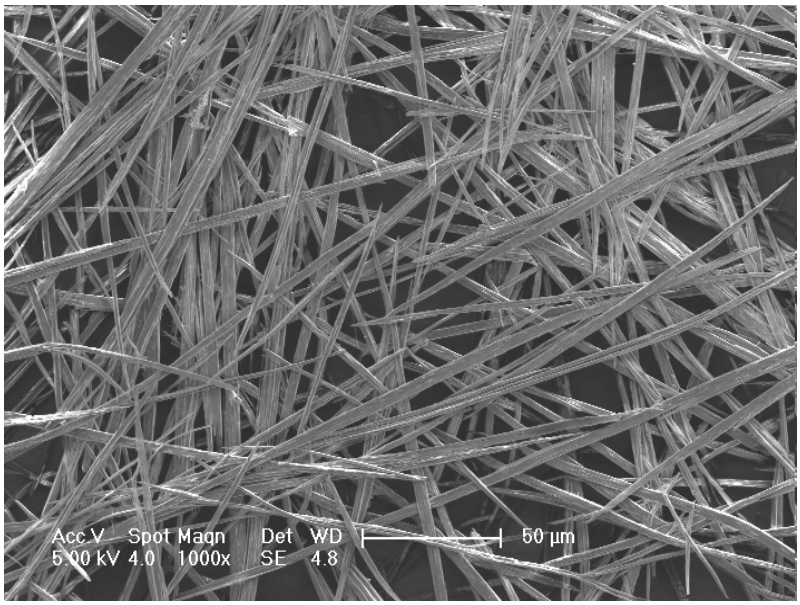

7.5. **Figure S7** SEM image of Racemic-**1** microstructure. The initial concentration of Racemic-**1** is 4×10^{-3} M **i**n MeOH. 0.5 ml of these solution was injected into high-purity water (2 mL) with vigorous stirring. After stirring 3 min, the sample was left undisturbed for about 8 h to stabilize the microstructures.

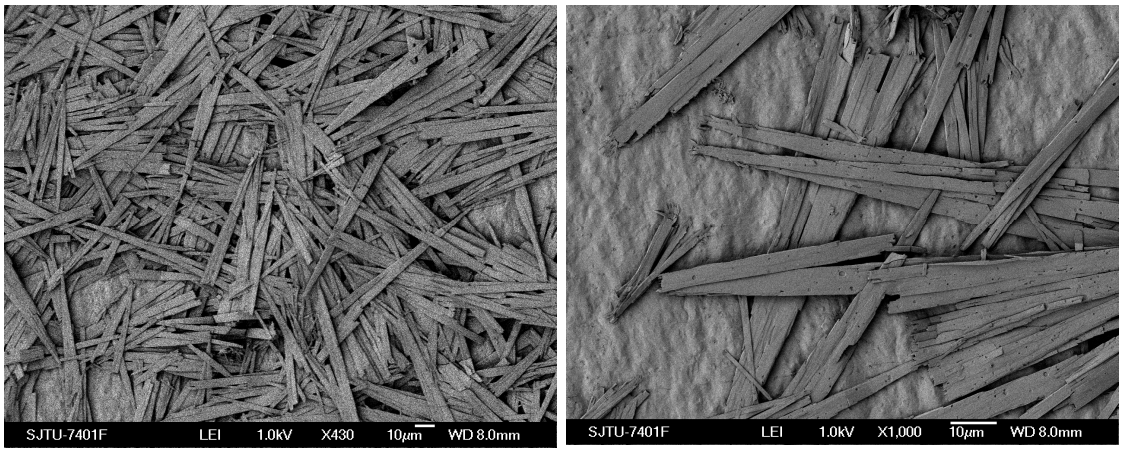

8. **Figure S8** Morphology evolution of *R*-**1**·2H_2O microleaves with the reaction time: SEM images of products obtained at room temperature for (a) 7 min, (b) 15 min, (c) 30 min, (d) and (e) 1 h, (f) 6 h. The possible formation mechanism of microleaves are also dissolution-recrystallization-induced concentration depletion. Similarity with the process of *R*-**1** microtubes at initial reaction stage, the spherical particles firstly transform into crystalline microrod. Once crystal growth begins, continual addition of molecules to the growing site along the preferred direction would form 1-D organic nanostructures. Then the dissolution of *R*-**1** by THF starts at the surface of the solid when all the molecules, except for those remaining solubilized, have participated to from 1-D nanostructures. However, recrystallization along the length axis also accompanies the "dissolution" process on the surface, and eventually the microrods turn into crystalline microleaves (S. T. Lee et al. *J. Phys. Chem. C* **2008,** 112, 16264-16268).

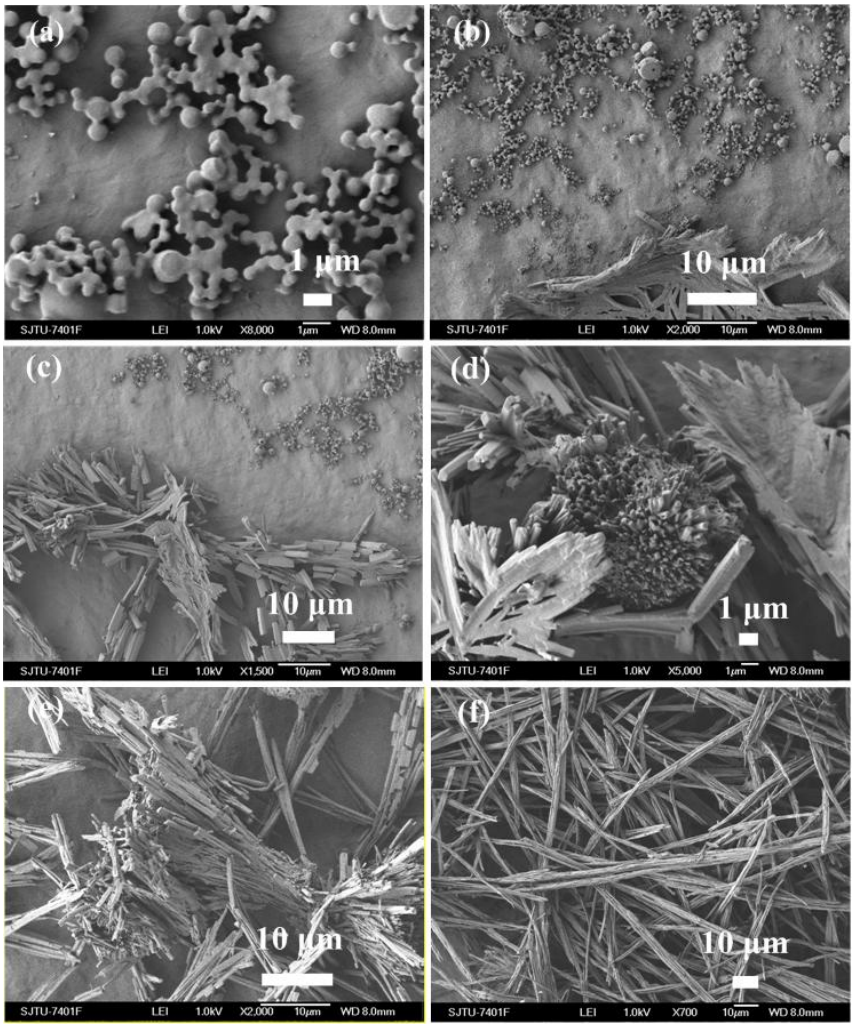

9.1. Figure S9. PXRD pattern of the starting material *R*-**1**, *R*-**1**·2H_2O obtained by exposing the starting material *R*-**1** to water vapor for 10 h, and the evacuated *R*-**1** by heating *R*-**1**·2H_2O under vacuum at 120 ^oC for 4 h.

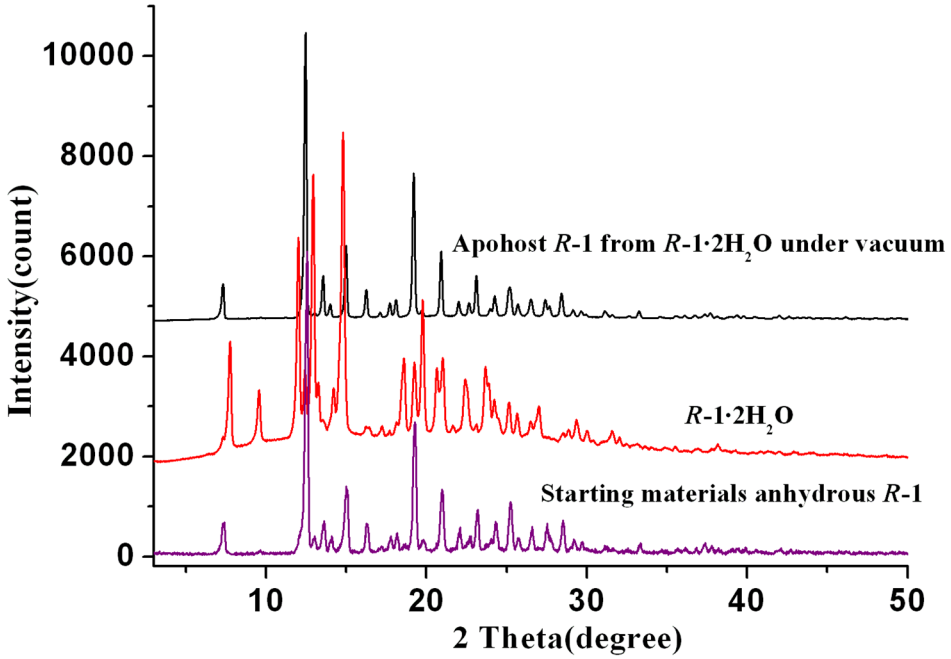

9.2. Figure S10. PXRD pattern of the products obtained at different reaction times (a, 5 min; b, 30 min; c, 10 h), and microspheres (d) and microleaves (e) and simulated PXRD of *R*-**1**·2H_2O (f).

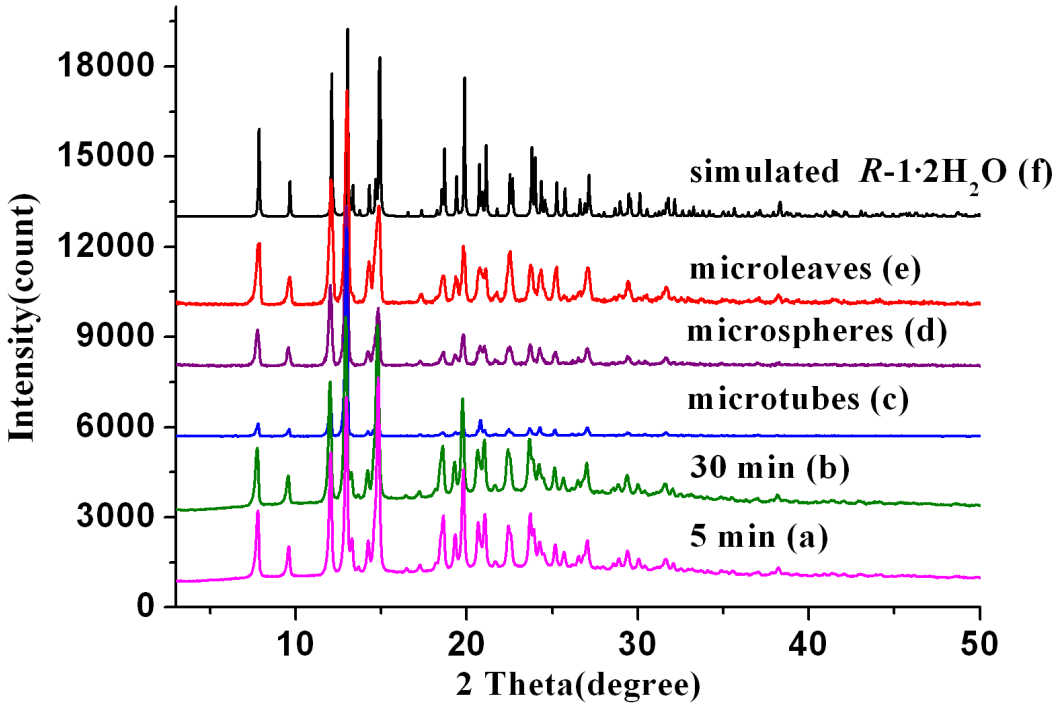

10.1 Figure S11. ^{1}H NMR spectra of anhydrous *R*-**1**, microtubes, microleaves and microspheres

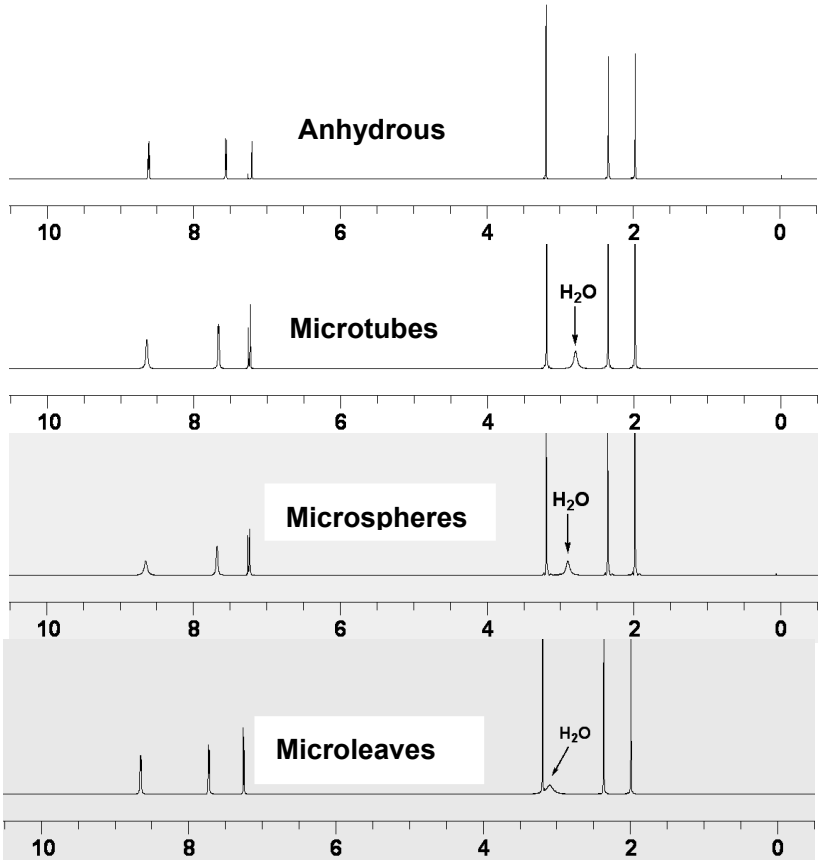

10.2 Figure S12. FTIR spectra of anhydrous *R*-**1**, microtubes, microleaves and microspheres

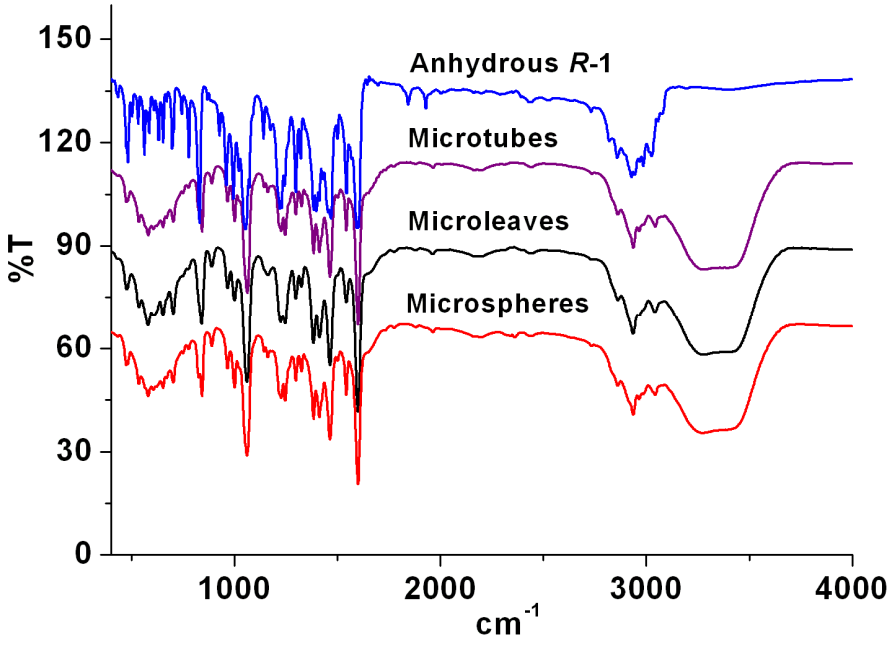

11.1. **Figure S13.** UV/Vis absorption spectra of *R*-**1**·2H_2O microstructures in the solid state at room temperature.

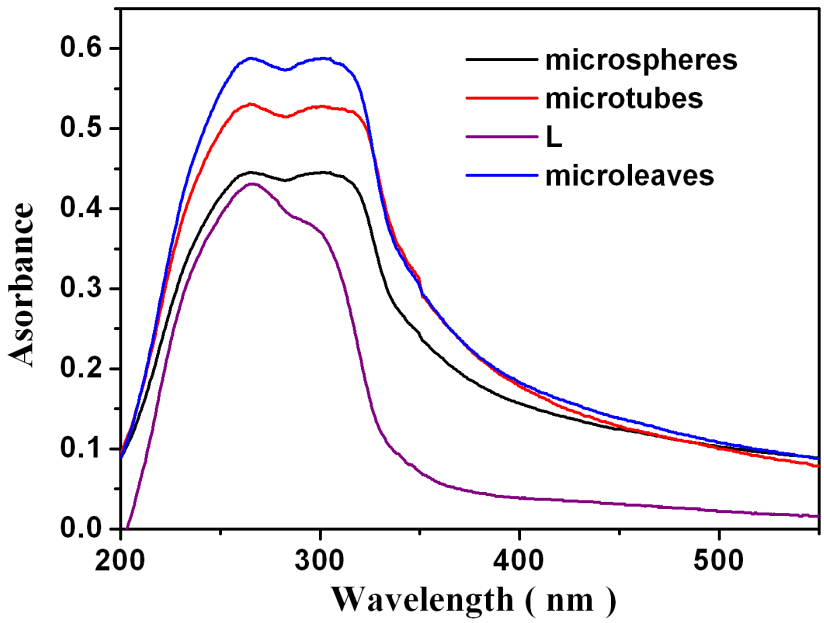

11.2. Figure S14. Fluorescent emission spectra of *R*-**1**(black) and *R*-**1**·2H_2O (red, the products were obtained by diffusing some distilled water into *R*-**1**) in the solid state at room temperature.

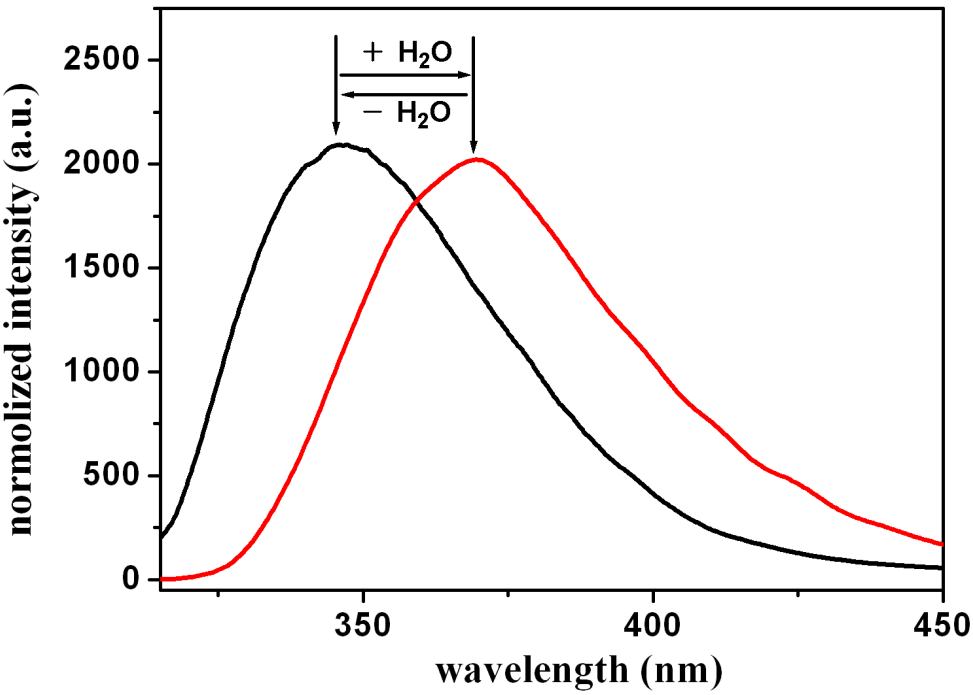

12.1 Figure S15. SEM images of (a) anhydrous powder *R*-**1**, (b) its hydrated powder after exposing in water vapor for 10 hours and (c) the re-evacuated sample obtained by heating the sample (b) under vacuum at 120 ^{o}C for 4 h.

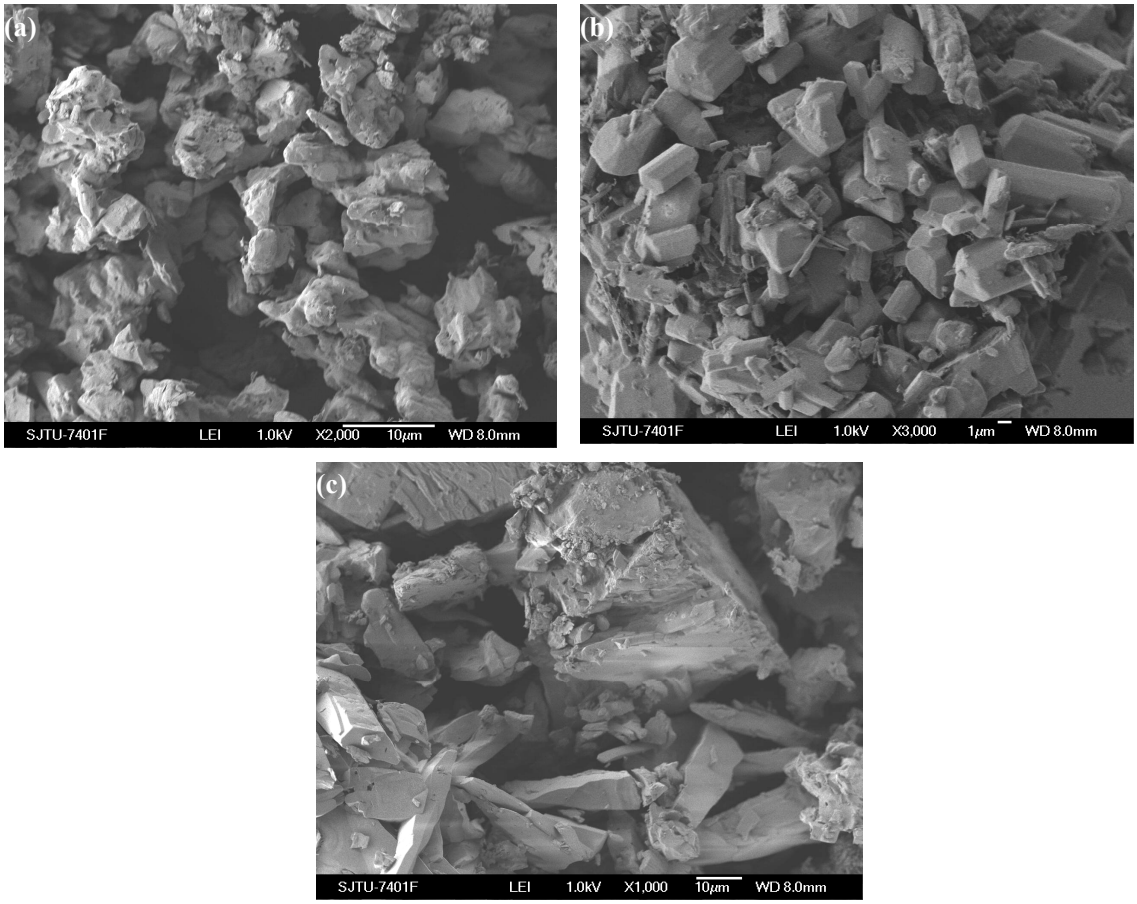

12.2. **Figure S16**. SEM images of (a) the anhydrous sample *R*-**1** obtained by heating microtubules under vacuum at 120 ^{o}C for 4 h and (b) its hydrated powder after after exposing in water vapor for 10 h.

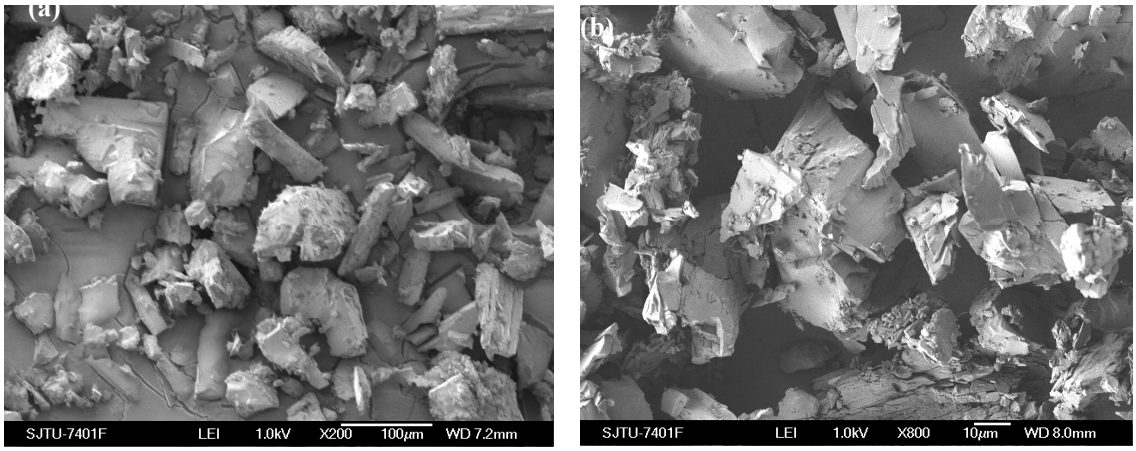

12.3. Figure S17. SEM images of (a) the anhydrous sample *R*-**1** obtained by heating microleaves under vacuum at 120 ^{o}C for 4 h and (b) its hydrated powder after after exposing in water vapor for 10 h.

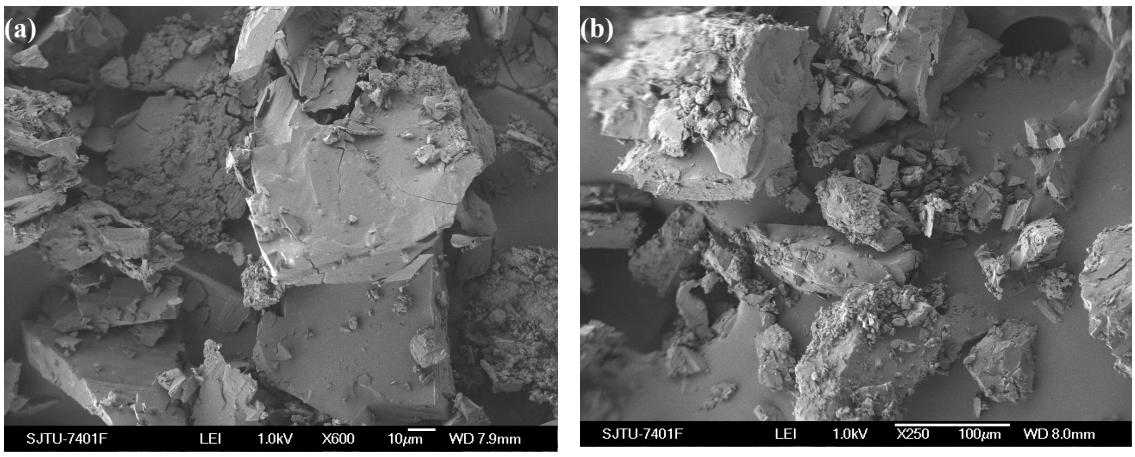

12.4. Figure S18. SEM images of (a) the anhydrous sample *R*-**1** obtained by heating microspheres under vacuum at 120 ^{o}C for 4 h and (b) its hydrated powder after after exposing in water vapor for 10 h.